Shock Waves (1995) 5:225–238

Shock Waves

Mechanisms of detonation transmission in layered H_2-O_2 mixtures

N.A. Tonello, M. Sichel, C.W. Kauffman

Department of Aerospace Engineering, The University of Michigan Ann Arbor, MI 48109, USA

Received August 1, 1993 / Accepted March 30, 1995

Abstract. When a plane detonation propagating through an explosive comes into contact with a bounding explosive, different types of diffraction patterns, which may result in the transmission of a detonation into the bounding mixture, are observed. The nature of these diffraction patterns and the mode of detonation transmission depend on the properties of the primary and bounding explosives. An experimental and analytical study of such diffractions, which are fundamental to many explosive applications, has been conducted in a two channel shock tube, using H_2-O_2 mixtures of different equivalence ratios as the primary and bounding or secondary explosive. The combination of mixtures was varied from rich primary / lean secondary to lean primary / rich secondary since the nature of the diffraction was found to depend on whether the Chapman-Jouguet velocity of the primary mixture, D_p, was greater than or less than that of the secondary mixture, D_s. Schlieren framing photographs of the different diffraction patterns were obtained and used to measure shock and oblique detonation wave angles and velocities for the different diffraction patterns, and these were compared with the results of a steady-state shock-polar solution of the diffraction problem. Two basic types of diffraction and modes of detonation reinitiation were observed. When $D_p > D_s$, an oblique shock connecting the primary detonation to an oblique detonation in the secondary mixture was observed. With $D_p < D_s$, two modes of reinitiation were observed. In some cases, ignition occurs behind the Mach reflection of the shock wave, which is transmitted into the secondary mixture when the primary detonation first comes into contact with it, from the walls of the shock tube. In other cases, a detonation is initiated in the secondary mixture when the reflected shock crosses the contact surface behind the incident detonation. These observed modes of Mach stem and contact surface ignition have also been observed in numerical simulations of layered detonation interactions, as has the combined oblique-shock oblique-detonation configuration when $D_p > D_s$. When $D_p > D_s$, the primary wave acts like a wedge moving into the secondary mixture with velocity D_p after steady state has been reached, a configuration which also arises in oblique-detonation ramjets and hypervelocity drivers.

Correspondence to: N. Tonello

Key words: Gaseous detonations, Detonative interactions, Layered detonations

1 Introduction

The refraction of a detonation propagating through a primary layer of gaseous explosive by a secondary bounding explosive or inert gas is of fundamental importance to many aspects of the propagation of detonations and reactive shock waves, and is the subject of this paper. This is the process which occurs when a detonation propagates from a detonation tube into a larger or unbounded medium, and the critical question is then whether or not the detonation will reignite and continue to propagate. This type of interaction is also involved in the propagation of detonations in layered explosives and represents many aspects of the propagation of detonations or reactive shocks past obstacles. In some cases, during this interaction, the primary detonation generates the equivalent of a wedge moving at high speed, resulting in the generation of oblique detonations in the bounding explosive similar to those which occur in oblique-detonation ramjets and hypervelocity drivers.

There have been a number of studies of this refraction process. Using nonreactive bounding mixtures, Sommers (1961) and Dabora (1963) studied the influence of a compressible boundary on the propagation of a detonation. Liu et al (1988) investigated the same interaction, but with an explosive as the bounding gas. An early shock-tube investigation and shock-polar analysis of such refractions was carried out by Gvozdeva (1961) and Gvozdeva and Predvoditeleva (1969). A shock-polar solution of this layered refraction was used by Liou (1986) to draw maps outlining different interaction regimes. Dabora et al (1991) used a layered shock-tube facility in which the primary gas and the secondary gas were separated by a mylar membrane in order to study oblique detonations at hypersonic velocities. Numerical simulations of detonation transmission into explosive or inert bounding layers have been carried out by Oran et al (1992). Observed wave structures resulting from these interactions were reproduced in these simulations, and ignition

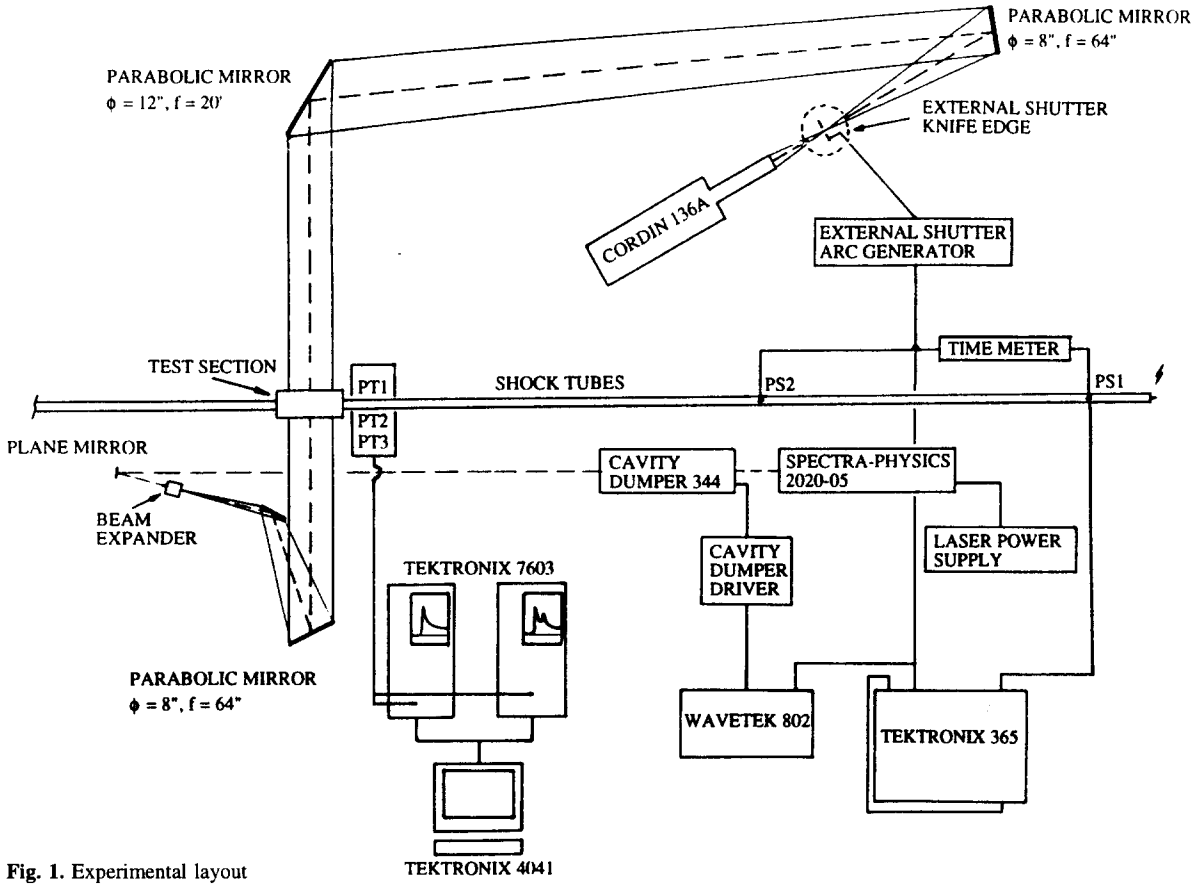

Fig. 1. Experimental layout

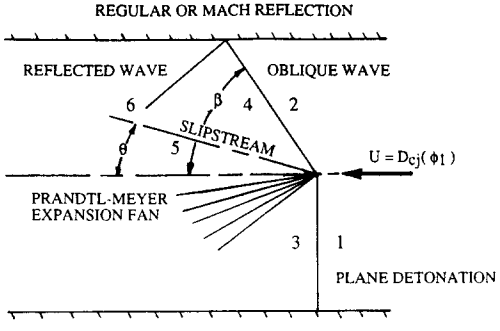

Fig. 2. Steady interaction in a reference frame fixed to the primary detonation wave

and quenching mechanisms were identified. The above studies showed that the nature of the refraction of the primary detonation wave by a bounding explosive mixture depended on whether the Chapman-Jouguet velocity of the primary mixture, D_p, was greater or less than that of the secondary mixture, D_s.

This paper presents the results of experiments carried out in a layered shock-tube, designed to study the interaction between explosive layers, with combinations of H_2-O_2 mixtures varying from a lean primary and rich secondary to rich primary and lean secondary mixtures. High-speed Schlieren framing photographs of the interactions were used to identify characteristic wave configurations and to measure the transmitted wave angles and wave speeds as a function of time. The propagation speeds of the primary and secondary waves were compared with the theoretical Chapman-Jouguet speeds computed using the Gordon-MacBride code (1971). The observed wave angles were compared to angles computed using steady-state shock-polar solutions. Two distinct modes of detonation ignition in the secondary mixture were observed when the primary explosive is lean, so that $D_p < D_s$. Oblique detonations are generated in the secondary mixture when the primary mixture is the richer one, so that $D_p > D_s$.

2 Experimental setup

The layered shock-tube used to obtain the results described here is shown schematically in Fig. 1. A detailed description of this facility is presented in other publications (Liu et al 1988). Two shock tubes, laid horizontally on top of each other, are filled independently with different gas mixtures. The two mixtures come into contact with each other in the test section, where they are no longer separated by a solid wall. Instead, to allow interaction between the two mixtures, but to avoid inter-diffusion, a very thin (50 nm) collodion separating membrane is used, similar to that used by Gvozdeva (1961) and Dabora (1963). The shock tubes are three meters long upstream of the test section, and have a 1.6 cm square cross sectional area. The test section is 20 cm long which, with the mixtures in use, provides an observation time of about 100 μs.

Schlieren pictures of the interaction are taken with a Cordin 136A high-speed rotating drum camera. Pulses of laser light are flashed through the glass test-section windows at 2 μs intervals to obtain a sequence of about 50

Table 1. Equivalence ratios and sound speeds combinations for the primary and secondary mixtures used in the experiments

Combinations		Lean / Rich			Stoic.	Rich / Lean		
Equivalence Ratios	ϕ_1	0.45	0.50	0.60	1.00	1.50	2.00	1.00
	ϕ_2	3.00	2.50	1.86	1.00	0.70	0.57	0.45
Sound speeds (m/s)	a_p	441.5	451.7	471.0	537.8	604.5	658.8	537.8
	a_s	743.1	704.2	644.6	537.8	489.2	465.4	441.5

Table 2. Comparison of the conditions behind a normal shock and an oblique shock traveling at Mach M_2 in the secondary mixture for different mixture combinations. Induction times and distances are computed for a normal shock. N/A: not available, pressure and temperature are such that explosive burning is ruled out

Equivalence ratios		Mach number	Mach number	(K) Temp.	(atm) Press.	(K) Temp.	(m/s) Speed	(μsec) Time	(mm) Dist.
ϕ_1	ϕ_2	M_1	M_2	T_{2n}	P_{2n}	T_{2o}	u_{2n}	t_i	d_i
0.45	3.00	5.10	3.04	792	10.4	551	569.4	N/A	N/A
0.50	2.50	5.15	3.30	900	12.7	565	554.0	N/A	N/A
0.60	1.86	5.20	3.80	1092	17.0	591	531.0	1.41	0.748
1.50	0.70	5.30	6.50	2437	50.6	700	513.5	0.02	0.010
2.00	0.57	5.20	7.32	2930	64.3	710	519.5	0.01	0.005
1.00	0.45	5.30	6.44	2414	50.7	698	709.1	0.02	0.015

framing photographs of the diffraction process for each run. This visualization technique provides a complete record for each experiment, in contrast to previous studies (Dabora 1963; Gvozdeva 1961) in which, typically, only one or a few Schlieren pictures could be obtained from each run. This technique eliminates the need to construct a complete record of the interaction by piecing together Schlieren pictures taken at different elapsed times from a whole sequence of tests made under the same conditions. The shock tube in which the primary detonation propagates is instrumented with Kistler 603B1 pressure transducers and pressure switches. The pressure signals are recorded and digitized with Tektronix 7603 oscilloscopes, and are also taped and analyzed with a Tektronix 4041 computer.

At the start of each experiment, a detonation is initiated in the primary explosive at the upstream end of the shock tube. In the experiments described below, the primary mixture is always in the bottom tube. When the detonation arrives at the test section, the burned gases behind the detonation expand into the secondary mixture, establishing a transmitted wave pattern. The detonation speed and pressure were measured using the instrumentation described above. As shown below, the measured speed of the primary detonation correlates extremely well with the theoretical Chapman-Jouguet velocity; the error relative to the computed speed never exceeding 2%. As is typical of detonation measurements, the measured pressures do not correlate as well with computed values, with the error varying between 7 and 16 %.

3 Mixture characteristics

As already indicated, experiments were conducted using H_2-O_2 mixtures for both the primary and secondary explosive, with various combinations of ϕ_1 and ϕ_2, the primary and secondary equivalence ratios, ranging from lean primary / rich secondary to rich primary / lean secondary, as listed in Table 1. The equivalence-ratio combinations were chosen so that the overall mixture ratio of the combined primary and secondary explosives was stoichiometric, with the exception of the combination $\phi_1/\phi_2 = 1.0/.45$, which therefore is listed last in Table 1. The choice of an overall stoichiometric mixture was dictated by the original intent of the investigation, which was to establish the effect of layering on detonation impulse.

The properties of the primary and secondary H_2-O_2 mixtures are listed in Table 2. $M_1 = D_p/a_p$ is the Mach No. of a C-J detonation propagating through the primary mixture, while $M_2 = D_p/a_s$ is the Mach No. of the flow ahead of the transmitted shock or detonation, assuming that the gas moves with the velocity of the primary wave. Here, a_p and a_s are the sound speeds in the primary and secondary explosives, and these are listed in Table 1. Thus, as ϕ_1 increases relative to ϕ_2, the CJ velocity D_p and a_p, the primary speed of sound, both increase, so that the Mach No. M_1 of the primary wave always remains at a value of about 5. However, as ϕ_2 decreases, the speed of sound a_s in the secondary mixture also decreases, so that the Mach No. M_2 increases as is evident from Table 2. The mixture ϕ_1/ϕ_2 for which the overall mixture ratio is not stoichiometric does not follow this sequence exactly, and so is listed last. T_{2n} and u_{2n} are the temperature and velocity behind a normal shock wave propagating through the secondary explosive at Mach No. M_2, while T_{2o} is the temperature behind an oblique transmitted-shock in the secondary mixture moving with velocity D_p.

Past studies have shown that the H_2-O_2 reaction is extremely temperature sensitive, and the induction or ignition delay time provides a measure of this sensitivity. For initial temperatures below 1100 K, a fast or slow reaction can take place depending on where the temperature–pressure coordinates of the mixture lie in relation to the explosive boundaries of the H_2O_2 system (Getzinger and Schott 1973). Above 1100 K, the fast reaction will always occur and an

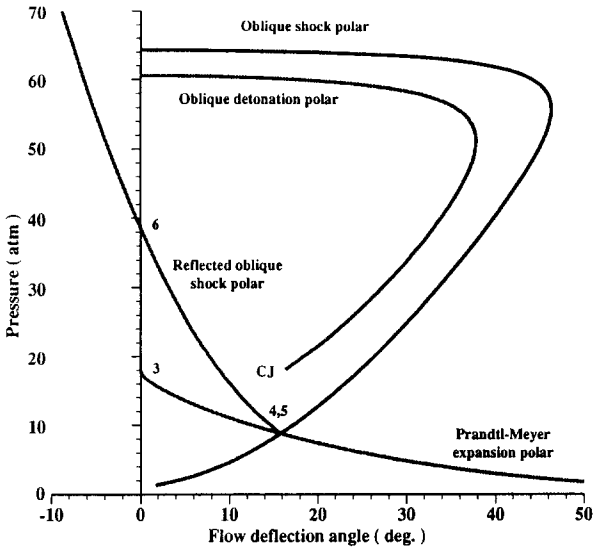

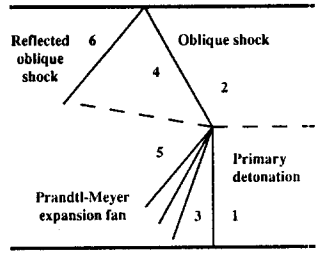

(a)

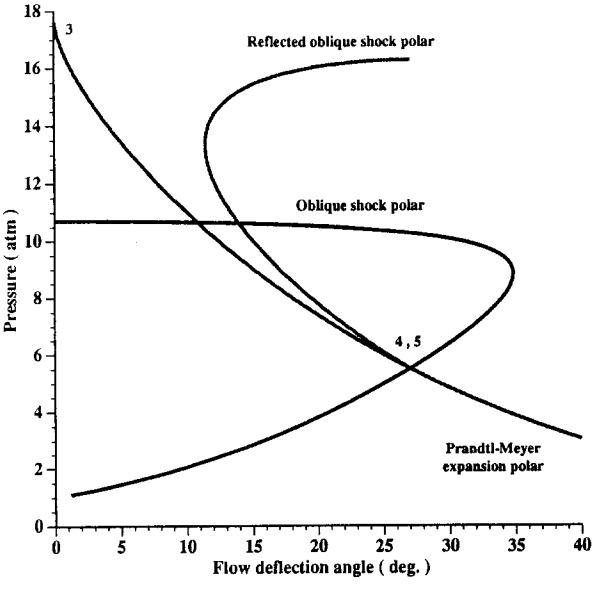

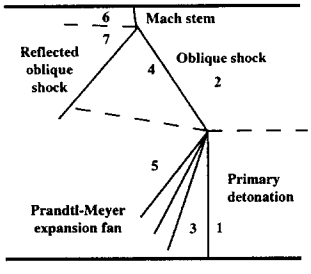

(b)

Fig. 3a,b. Pressure polars for the steady state diffraction problem with rich primary and lean secondary explosives, (ϕ_1 = 2.0)/(ϕ_2 = 0.57); Pressure polars for the steady-state diffraction problem with lean primary and rich secondary explosives, (ϕ_1 = 0.45)/(ϕ_2 = 3.0)

induction time t_i can be computed (White and Moore 1965) from the empirical relation:

$$\log_{10}\left(\sqrt{[O_2][H_2]}t_i\right) = \frac{3100}{T} - 9.8\,,$$

where $[O_2]$ and $[H_2]$ are concentrations. The induction time based on this expression is, thus, a function of the temperature, pressure, and equivalence ratio ϕ.

In order to obtain a measure of the sensitivity of the secondary mixture for the experiments described below, the induction time t_i and the induction distance $d = u_{2n}t_i$ have been computed using the above relation at conditions corresponding to temperature T_{2n} and the velocity u_{2n} behind a normal shock wave propagating with Mach No. M_2 through the secondary mixture, and these are also presented in Table 2. Since there is no guarantee that the White-Moore (1965) relation remains valid at the high values of P_{2n}, these values must be considered as only providing a qualitative indication.

It can be seen that T_{2n} increases as ϕ_1 increases relative to ϕ_2, so that t_i and hence d decrease drastically, with a consequent increase in the sensitivity of the secondary mixture. As will be seen from the experimental results described below, there is a complete change in the nature of the diffraction process and the mechanisms by which a detonation is ignited in the bounding mixture, as ϕ_1 increases from lean to rich values. When an oblique shock is transmitted into the bounding mixture, the temperature T_{2o} behind it, which also is presented in Table 2, is considerably below T_{2n}, so that direct initiation of combustion behind oblique shocks is unlikely.

4 Steady-state analysis

Assuming that the interaction has reached a steady state, the wave system consisting of the primary detonation wave and the transmitted waves travels horizontally at the speed of the primary detonation. The resultant configuration can, then, be analyzed using shock polars based on a stationary reference frame fixed to the primary detonation. A sketch of a typical refraction pattern is shown in Fig. 2 for the case in which $D_p > D_s$. Then, the combustion products behind the primary detonation expand through a Prandtl-Meyer wave, while the unburned secondary mixture is compressed by a transmitted wave which may be an oblique shock or detonation. The wave angle β of the transmitted wave can be determined by imposing the condition that the pressure and flow angle on the two sides of the slipstream or contact surface, between the expanded and burned primary gas and the shocked or detonated secondary gas, must be equal so that:

$$P_4 = P_5; \quad \theta_4 = \theta_5$$

State 3 is assumed to correspond to that at the Chapman-Jouguet plane so that P_3 is the Chapman-Jouguet pressure and the flow is sonic. To compute the pressure and the flow deflection angle behind the transmitted wave the conservation equations must be solved across the wave. Solutions were obtained for either a chemically-frozen oblique shock wave or an oblique detonation wave, using the two-gamma method presented in detail by Liou (1986) and described briefly below.

To take vibrational excitation and dissociation into account, the secondary gas is assumed to be ideal on both sides of the transmitted wave, but with different values of the ratios of specific heats k_2 and k_4. The enthalpies and sound speeds on both sides of the wave are computed with average specific heat ratios k_2 and k_4. The specific heat ratio k_2 of the unburned secondary explosive is equal to the isentropic exponent γ_2. When the transmitted wave is a chemically-frozen shock, k_4 is computed as a function of C_{p4}, the average specific heat at temperature T_4, computed using the Gordon-McBride code (1971). When the transmitted wave is an oblique detonation, k_4 is taken to be equal to γ_{S4}, the isentropic exponent behind a Chapman-Jouguet detonation as determined from the Gordon-MacBride code (1971). The isentropic exponent is generally not equal to the ratio of specific heats and is defined by the relation:

$$\gamma_S = \left(\frac{\partial \ln P}{\partial \ln \rho} \right)_S .$$

As shown by Liou (1986), this choice for k_2 and k_4 gives results almost identical to exact detonation polar calculations based on the Gordon-MacBride code (1971).

Since analytical formulas for the wave angles could not be found, a graphical method of solution based on shock and detonation polars was used. A similar analysis was used by Gvozdeva and Predvoditeleva (1969). Polar plots for a transmitted frozen shock and for a transmitted oblique detonation were drawn, corresponding to the propagation velocity D_p of the primary detonation. The polar corresponding to a Prandtl-Meyer (P-M) expansion behind the primary detonation was plotted on the same figure. Two typical polar plots are shown in Figs. 3(a) and (b). Figure 3(a) shows polars for the case in which the primary mixture is rich, with an equivalence ratio $\phi_1 = 2.0$, while the secondary mixture is lean, with $\phi_2 = 0.57$. In this case, the CJ velocity in the primary mixture is greater than that in the secondary mixture, that is $D_p > D_s$. From Table 2 it can be seen that the Mach No. $M_1 = D_p/a_1 = 5.20$, while the Mach No. $M_2 = D_p/a_2 = 7.32$, and it is this latter Mach No. which determines the transmitted shock and detonation polars shown in Fig. 3(a). Figure 3(b) shows polars for the case in which the primary mixture is lean, with an equivalence ratio $\phi_1 = 0.45$, while the secondary mixture is rich, with $\phi_2 = 3.0$. The CJ velocity in the primary mixture is now lower than that in the secondary mixture and, as evidenced in Table 2, the Mach No. M_2 is too low for an oblique detonation to exist in the secondary mixture. In this case, polars can be drawn only for the transmitted and reflected shocks, in addition to the expansion wave behind the primary detonation.

When it exists, the oblique detonation polar always lies inside the corresponding oblique shock polar, but is not closed. The terminal point shown in Fig. 3(a), labeled CJ, corresponds to a Chapman-Jouguet oblique detonation for which the normal component of the velocity ahead of the waves equals the C-J velocity D_s of the secondary explosive, while the normal component of the velocity downstream of the detonation is sonic. A property of the H_2-O_2 system is that the pressure in the C-J plane varies little with the mixture ratio. This means that, for all possible combinations of primary and secondary mixture ratios, the point labeled CJ in Fig. 3(a) is almost on the same horizontal line as the point labeled 3, but offset from it because of the difference in flow deflections angles at points CJ and 3. But in the marginal case where both primary and secondary mixtures are stoichiometric, the oblique detonation and Prandtl-Meyer expansion polars can, therefore, not cross.

From this it follows that, in the H_2-O_2 system, steady-state configurations in which the transmitted wave is an oblique detonation cannot exist even when $D_p > D_s$; rather, the transmitted wave will be an oblique shock determined by the intersection of the oblique shock polar and Prandtl-Meyer polar, as shown in Fig. 3(a). When $D_p > D_s$, oblique shocks are generated in the secondary explosive, in fact, as indicated below, the transmitted wave often takes the form of a oblique shock-oblique, detonation-complex, as discussed in detail below.

Because of the properties of the H_2-O_2 system, the P-M expansion polar always lies below the CJ point of the oblique detonation polar, and there will, then, also be an expansion wave behind any oblique detonations generated in the secondary mixture. As a consequence, the oblique detonation angles computed here for comparison with the measured values always correspond to those of the CJ oblique detonation in the secondary explosive. A detailed analysis of a wide range of steady-state interaction configurations based on the shock polar analysis described above has been presented by Liou (1986).

Once the solution for the transmitted wave is determined, it is possible to draw a polar for the reflected shock required to align the flow with the top wall of the secondary channel. In the case of regular reflection, the reflected shock angle is found at the point where the reflected shock polar crosses the ordinate axis and there is zero absolute flow deflection with regard to the wall, as shown by point 6 in Fig. 3(a). When, as in Fig. 3(b), the reflected shock polar does not cross the ordinate axis, the detachment criterion dictates that a Mach stem is to be expected at the top wall.

5 Experimental results

Experimental results for a number of the mixture combinations listed in Table 2 are described in detail below. For each case, a sequence of Schlieren framing photographs is presented, showing the evolution of the diffraction with time. Each photograph is accompanied by an explanatory sketch. On the photographs, the waves propagate from left to right, and, as already indicated above, the primary mixture is always on the bottom. In each case, the observed velocities and wave angles are compared with those computed using the steady-state analysis described above.

5.1 Lean primary / rich secondary

Direct ignition of the secondary mixture was not observed with this combination of mixtures, as is to be expected from the discussion of t_i and d above. The secondary mixture ignites either behind the Mach stem resulting from the reflection of the transmitted shock from the top wall of the test section, or along the slipstream or contact surface (shown

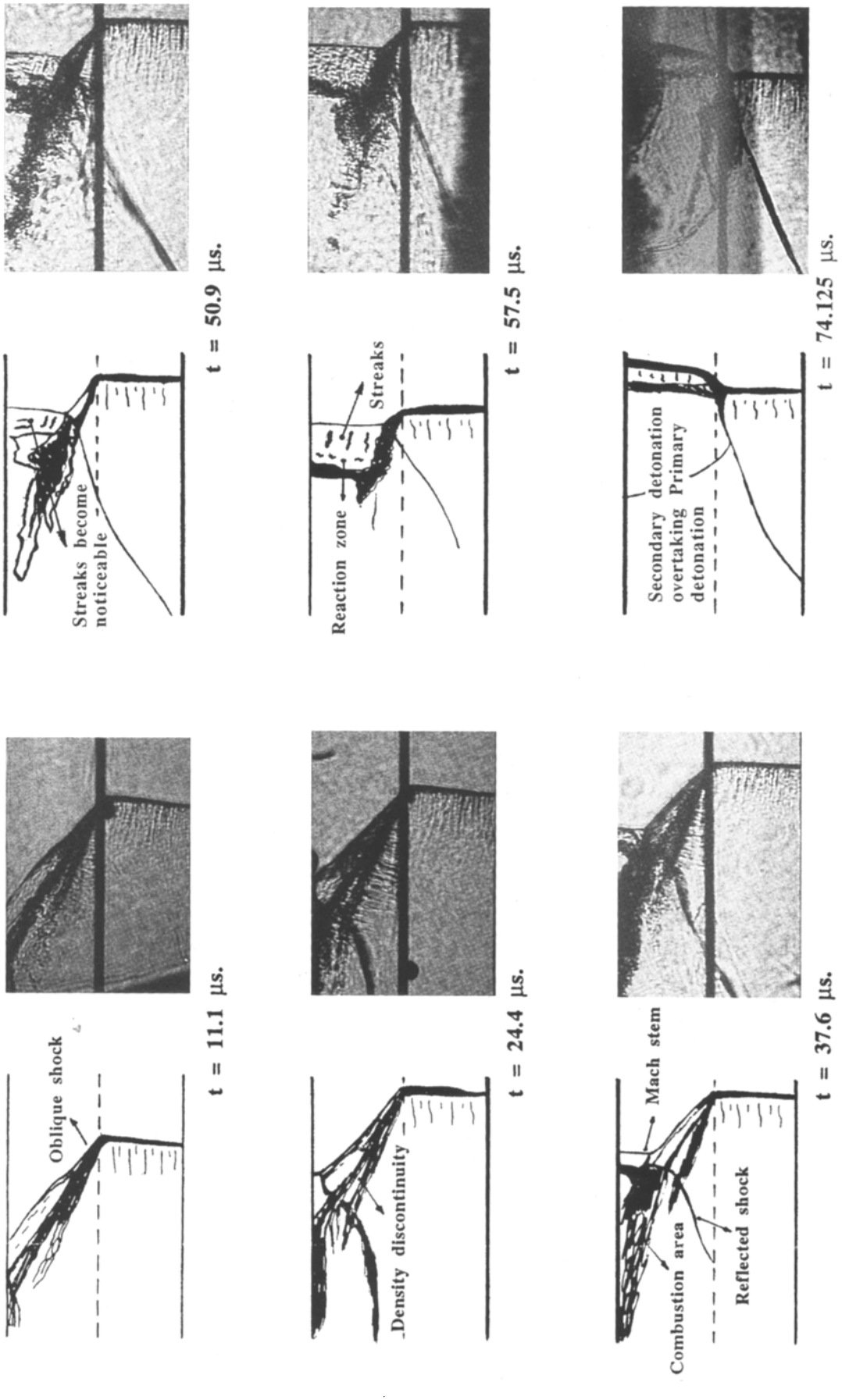

Fig. 4. Schlieren photographs and sketches of the interaction; $\phi_1 = 0.45$, $\phi_2 = 3.0$

in Fig. 2), after the slipstream crosses the reflection of the transmitted oblique shock.

Mach stem ignition was observed in the case where $\phi_1 = 0.45$ and $\phi_2 = 3.0$, for which selected framing photos at different values of elapsed time are shown in Fig. 4. At the beginning of the interaction, a blast bubble or wave attached to the primary detonation, which is not shown in Fig. 4, propagates into the secondary mixture. As it propagates, this blast wave evolves into an oblique shock which may have a kink or slight discontinuity in slope, as shown in the frame for 11.1 μs. Above this kink the wave can be either curved or straight with a larger slope than the lower segment. An oblique density discontinuity, which is probably the slipstream separating the combustion products behind the primary wave and the unburned secondary mixture behind the oblique shock, can be observed between this oblique shock and the lower channel at $t = 11.1$, 24.4, and 37.6 μs. This discontinuity splits into two branches at approximately the middle of the secondary region, for reasons which are not entirely clear. This split could, conceivably, be a result of the fact that the experiment is not truly two-dimensional. But this second density front also could be caused by reaction within the secondary explosive between the oblique shock and the slipstream.

The transmitted oblique shock angle is such that Mach reflection is observed at the upper test section wall at 24.4 μs. The reflected shock can be seen to intersect the two branches of the density discontinuity at 24.4 and 37.6 μs. The lower branch of this discontinuity disappears between 37.6 and 50.9 μs, just after it has been turned by the reflected shock. The upper branch of the density front is deflected downward by the reflected shock and remains visible until it runs almost parallel to the top wall and intersects with it at 50.9 μs. At 24.4 and 37.6 μs, the upper wall, the reflected shock, and the upper branch of the density front bound a region where the many changes in contrast on the Schlieren photographs imply that there are strong density variations in this region. It can be argued that the part of the upper branch of the density front outside the reflected shock marks the limit between shocked and burning secondary gas.

When combustion appears behind it, at 37.6 μs, the Mach stem starts growing at an accelerated rate. The overall configuration is the same as at 24.4 μs, but the Mach stem is much bigger than before and a straight contact surface parallel to and behind it, which is probably a combustion front, has appeared. The combustion region between the wall and the upper branch of the density front behind the reflected shock is still fairly thick and extends a long way towards the wall. As the Mach stem continues to grow, the combustion region behind the reflected shock shrinks (50.9 μs). At 57.9 μs, the vertical contact surface is still at some distance behind the Mach stem and does not appear to be coupled to it. Finally, as shown in the last sketch in Fig. 4, the Mach stem, which is very close to or may actually be a plane detonation, overtakes the primary detonation wave. The secondary detonation then takes the lead, as is to be expected since $D_s > D_p$, and what was originally the planar primary detonation evolves into a combination of oblique and planar detonations. A complete picture of this type of transition is shown in Fig. 6 for $\phi_1/\phi_2 = 0.6/1.86$ and is discussed in detail below. Essentially, ignition of the secondary mixture has occurred by Mach reflection.

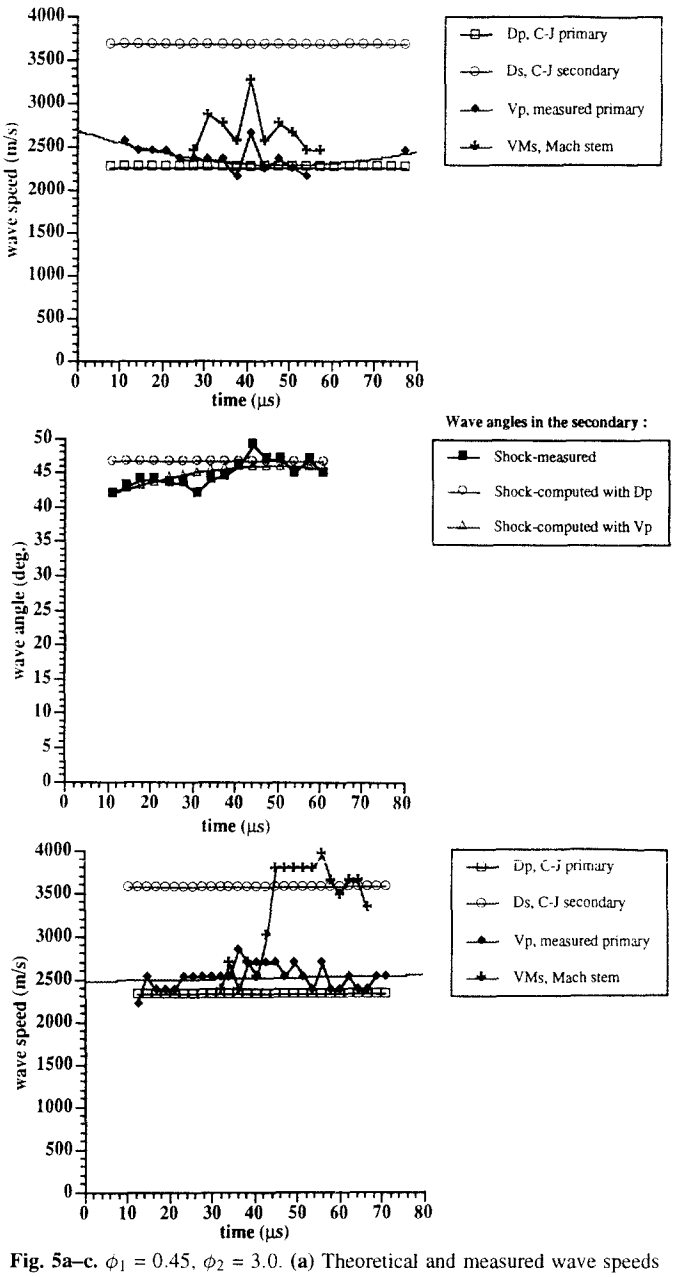

Fig. 5a–c. $\phi_1 = 0.45$, $\phi_2 = 3.0$. **(a)** Theoretical and measured wave speeds versus time; **(b)** measured and computed wave angles versus time; **(c)**: $\phi_1 = 0.5$, $\phi_2 = 2.5$. Variation of theoretical and measured propagation velocity with time

Computed and measured wave velocities are compared in Fig. 5(a). It can be seen that, initially, the measured value of the primary wave velocity V_p is greater than the computed CJ velocity D_p, but then stabilizes around the theoretical value. Based on data from Ben-Dor (1978) and Lee (1984) from non-stationary shock-diffraction experiments in a diatomic ideal gas with an oblique shock angle of 45 degrees, which is about the value observed here, it is to be expected that Mach reflection will occur. Using the triple-point trajectory angle obtained from this data, the Mach stem speed should be about 2500 m/s when the detonation travels at $V_p = 2400$ m/s. The measured Mach stem velocity VMs was greater than this value, but lower than the CJ velocity D_s of the secondary mixture. This suggests that there was combustion

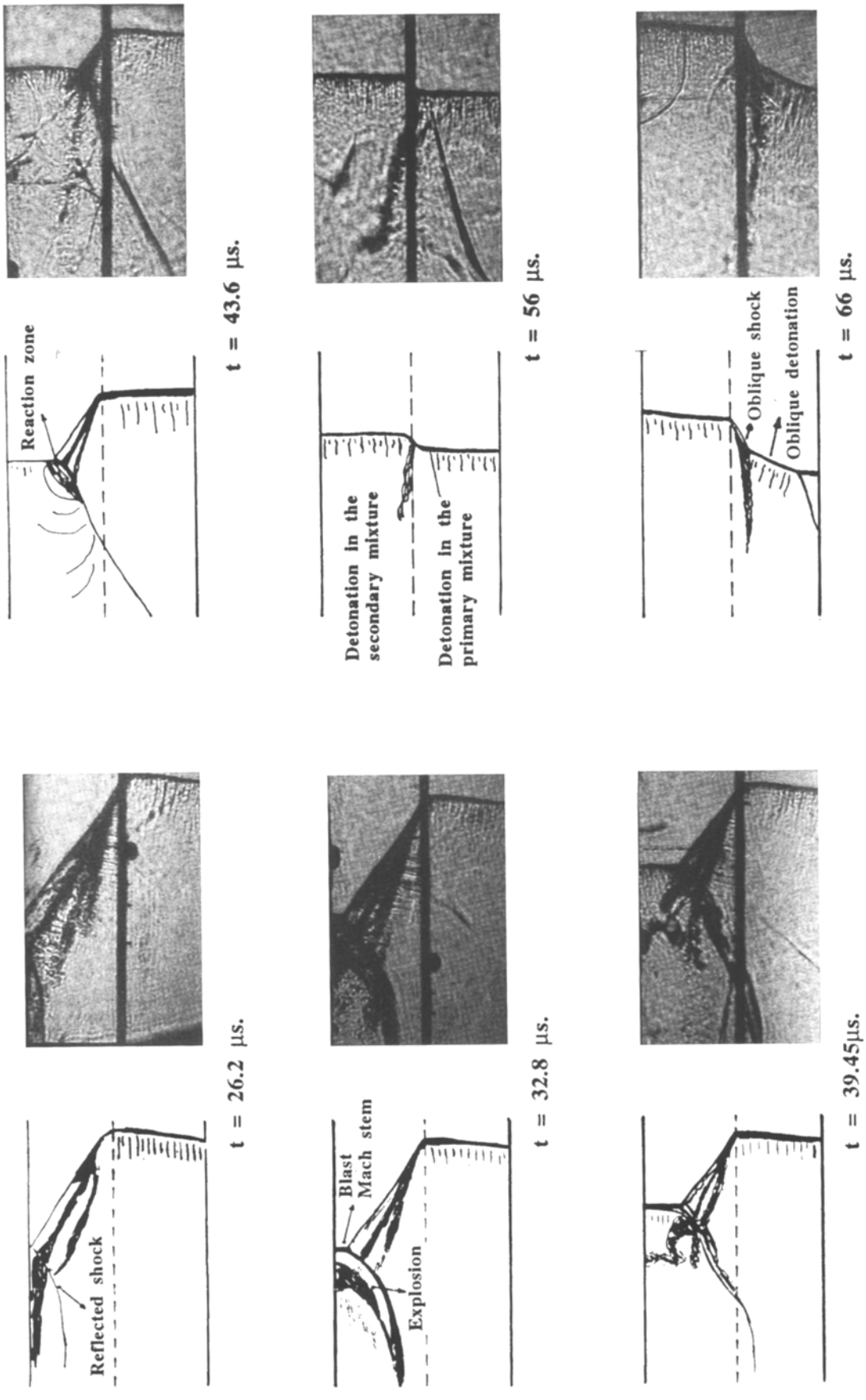

Fig. 6. Schlieren photographs and sketches of the interaction; $\phi_1 = 0.6$, $\phi_2 = 1.86$

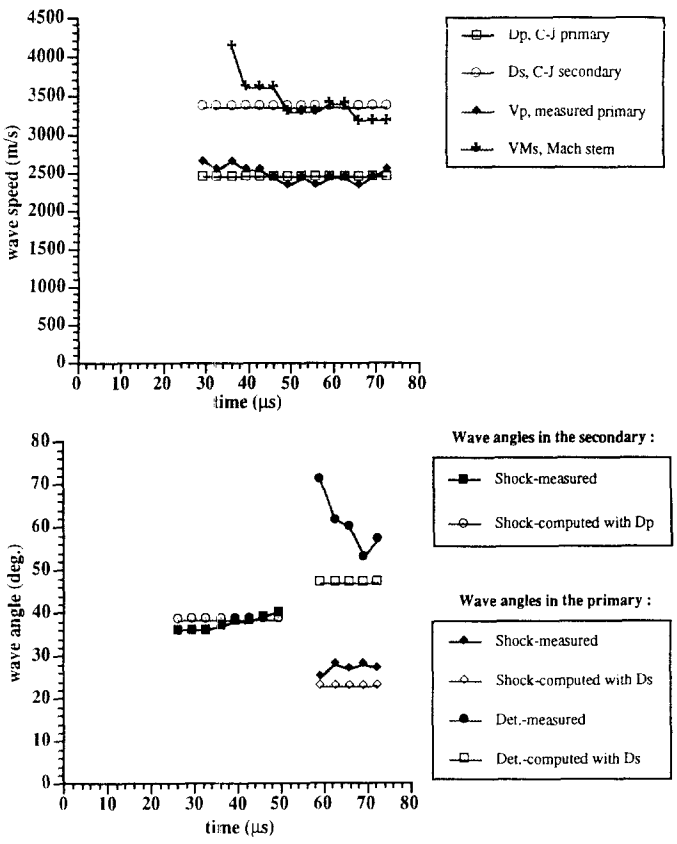

Fig. 7a,b. $\phi_1 = 0.6$, $\phi_2 = 1.86$. **(a)** Theoretical and measured wave speeds versus time; **(b)** measured and computed wave angles versus time

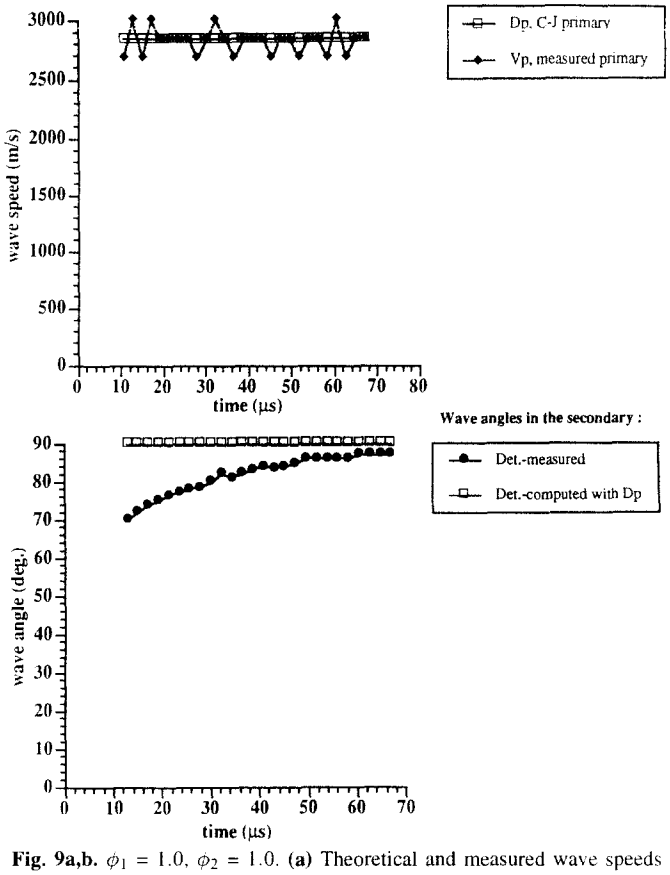

Fig. 9a,b. $\phi_1 = 1.0$, $\phi_2 = 1.0$. **(a)** Theoretical and measured wave speeds versus time; **(b)** measured and computed wave angles versus time

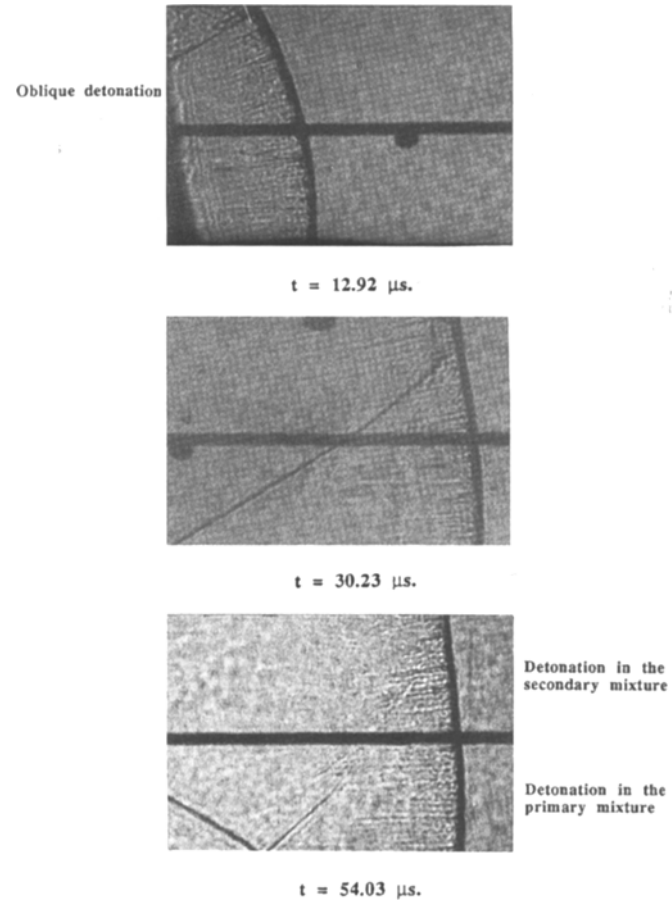

Fig. 8. Schlieren photographs of the interaction: $\phi_1 = 1.0$, $\phi_2 = 1.0$

behind the Mach stem but not transition to detonation, as was to be expected because of the large distance between the contact surface and the Mach stem observed at 57.5 μs. Figure 5(c) shows measured and computed velocities for $\phi_1/\phi_2 = 0.5/2.5$, and, here, it can be seen that the Mach Stem velocity VMs accelerates from the primary detonation velocity D_p to the secondary velocity D_s, at an elapsed time of about 45 μs. This suggests that transition of the Mach stem to a full-fledged detonation has occurred. This no doubt reflects the increase of T_{2n} from 792 K for $\phi_1/\phi_2 = 0.45/3.0$ to 900 K for $\phi_1/\phi_2 = 0.5/2.5$, with a resultant increase in the sensitivity of the secondary mixture.

Measured oblique-shock angles in the secondary mixture and values computed using the observed primary wave speed V_p and the primary CJ velocity D_p are shown in Fig. 5(b). The shock angles computed using V_p and D_p are in good agreement with the measured values. From the steady-state calculations, the deflection angle of the slipstream or contact surface was found to be 26°, which corresponds to the angle of the lower branch of the density discontinuity in the framing photographs. This confirms that this branch is, in all likelihood, the boundary between the burned primary combustion products and the unburned secondary explosive.

The calculated gas temperature behind the transmitted oblique shock is 551 K, while the temperature behind a normal frozen shock traveling in the secondary mixture at the primary CJ speed D_p of 2257 m/s is 792 K (Table 2). These relatively low temperatures explain why direct or violent ignition immediately behind the transmitted shock or Mach stem does not occur in this run.

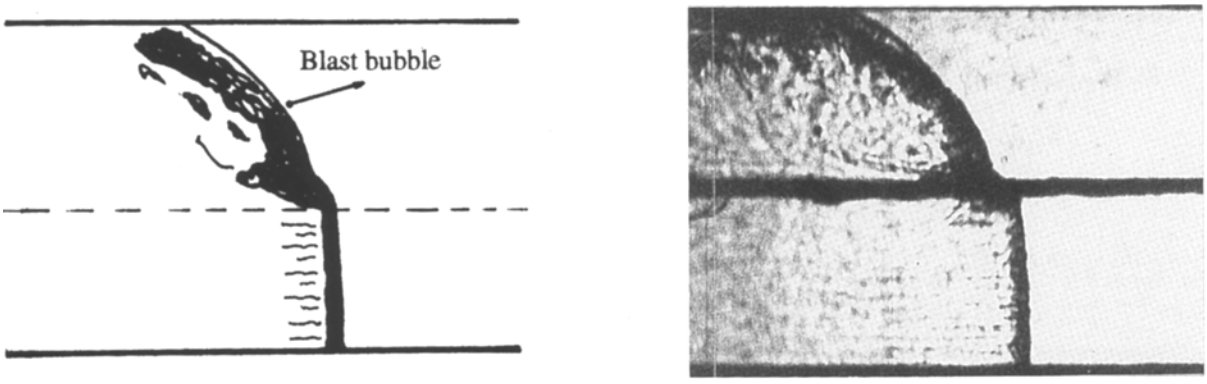

t = 12.6 μs.

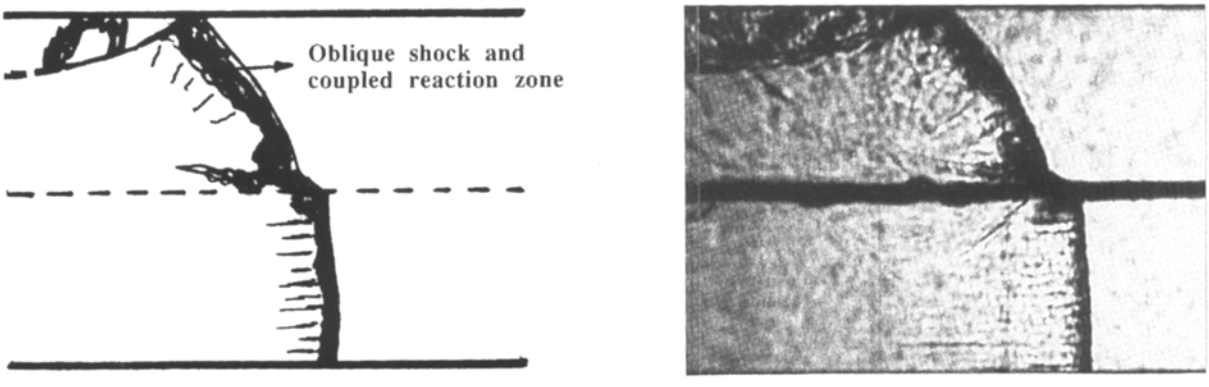

t = 15 μs.

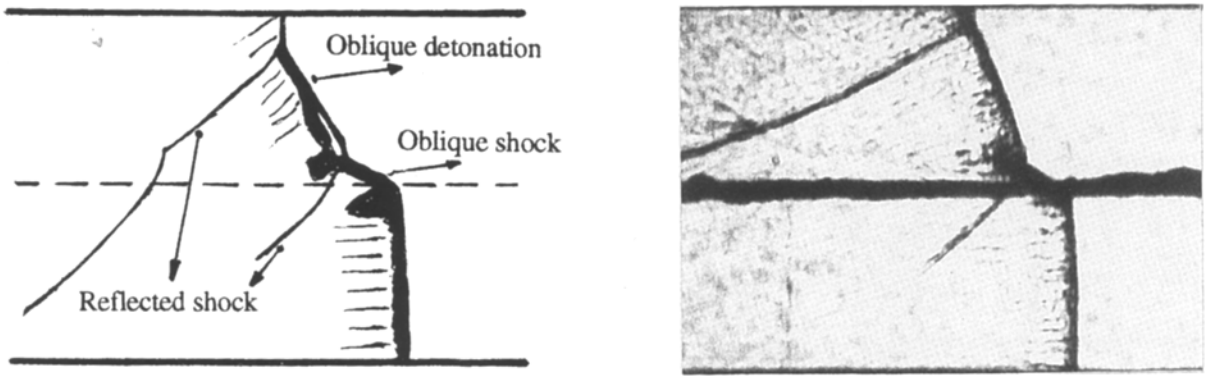

t = 22.2 μs

Fig. 10. Schlieren photographs and sketches of the interaction; $\phi_1 = 1.0$, $\phi_2 = 0.45$

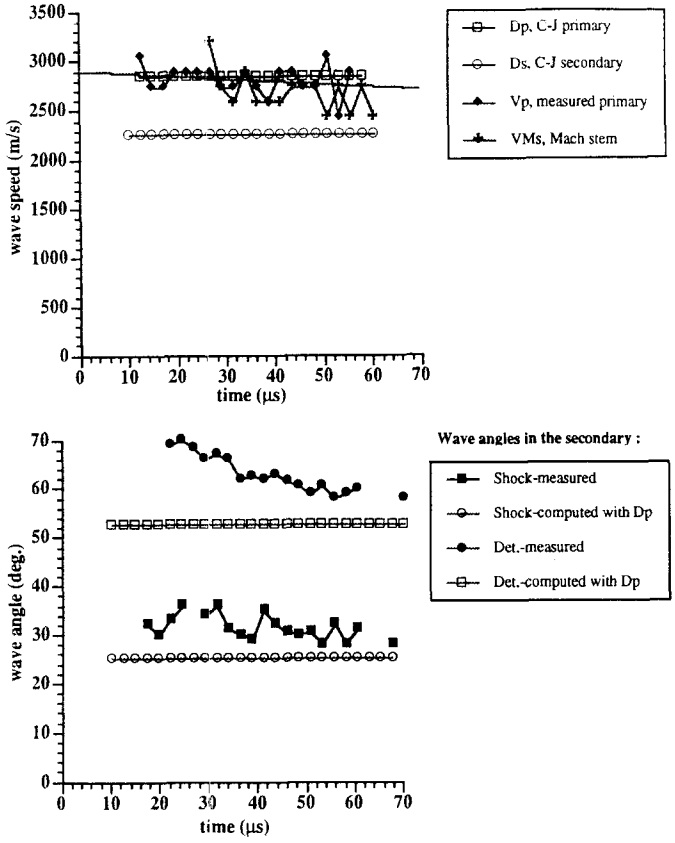

Fig. 11a,b. $\phi_1 = 1.0$, $\phi_2 = 0.45$. **(a)** Theoretical and measured wave speeds versus time; **(b)** measured and computed wave angles versus time

The results for $\phi_1 = 0.5$ and $\phi_2 = 2.5$ are similar to those described above and are not shown here. A Mach reflection of the transmitted oblique shock again occurs at the upper wall. Now, however, the Mach No. M_2 relative to the oblique shock has increased from 3.04 to 3.3, and the normal and oblique shock temperatures T_{2n} and T_{2o} have increased from 792 K and 551 K to 900 K and 565 K. The mixture behind the Mach stem is, consequently, much more sensitive. As a result, the vertical reaction front described above and the Mach stem rapidly become coupled, and, after an elapsed time of about 50 μs, the Mach stem velocity jumps from D_p to D_s, the secondary CJ velocity. The Mach stem has clearly become a detonation propagating at the secondary CJ velocity, and rapidly overtakes the primary detonation. The ignition which initiates this process seems to occur at the point where the reflected shock crosses the contact surface or slipstream behind the transmitted oblique shock. This mode of ignition is definitely involved in the case $\phi_1/\phi_2 = 0.6/1.86$, which is now discussed in detail.

Framing photos for $\phi_1 = 0.6$ and $\phi_2 = 1.86$ are shown in Fig. 6. The angle of the transmitted oblique shock is now too small for Mach reflection to occur, as is evident at 26.2 μs. Instead of slow combustion behind the Mach stem, as in the former cases, explosive ignition takes place at 32.8 μs behind the reflected shock, where the upper branch of the density discontinuity or contact surface crosses the reflection of the transmitted shock. This mode of ignition has also been observed in numerical simulations of reflected shock ignition by Jones at al (1995). The resulting blast wave overtakes the reflected shock, causing it to steepen, and a "Blast Mach stem" appears. Usually, as at 39.45 μs, this Mach stem has clearly developed into a planar detonation. At 56 μs, the Mach stem detonation has overtaken the primary detonation, as in the case for $\phi_1/\phi_2 = 0.5/2.5$ described above.

The measured primary wave speed V_p, shown in Fig. 7(a), is almost identical with D_p. The early ignition of the Mach stem in the secondary mixture is evident and its velocity VMs rapidly approaches D_s, the secondary CJ speed. The primary detonation velocity is not affected by the explosion in the secondary mixture. The measured and computed oblique shock angles, shown in Fig. 7(b), are in excellent agreement.

Halfway through the run, at about 50 μs, the secondary detonation takes the lead, so that the diffraction actually shifts from lean-rich to rich-lean and the primary mixture on the bottom takes on the role of the secondary explosive. A combined oblique-shock oblique-detonation wave, which is discussed in more detail below, is then transmitted into the bottom mixture. Oblique shock and detonation angles computed using D_s are compared to measured values in Fig. 7(b), for $t > 50$ μs. The measured oblique-shock angle rapidly approaches the computed value, but remains slightly greater, which correlates well with the fact that the actual speed of the secondary detonation lies somewhat below the CJ value. The oblique detonation angle seems to be converging towards the computed value, from above.

The computed temperature T_{2o} behind the transmitted oblique shock with a theoretical shock angle of $\beta = 38.3°$ is 591 K and the velocity of the fluid behind the shock is 1977 m/s. Thus, ignition directly behind the transmitted shock is highly unlikely. Behind the reflected shock, the calculated temperature is 915 K and the velocity is 1281 m/s. This combination of high speed and relatively low temperature explains why ignition occurs at a considerable distance from the reflected shock and why the reaction front does not instantly couple with the shock to form a detonation. Rather, the explosion at the intersection of the reflected shock and the contact surface generates a blast wave that strengthens the reflected shock; a Mach stem then develops, and fast reaction can take place behind the reflected shock and the Mach stem, where the induction distance d is of the order of 0.75 mm (Table 2). The secondary mixture, therefore, appears to ignite after the shocked secondary gas is heated by contact or mixing with the primary burned gas at the contact surface and, subsequently, passes through the reflected shock.

5.2 Stoichiometric primary / stoichiometric secondary

The diffraction which occurs when both the primary and the secondary mixtures are stoichiometric is shown in Fig. 8. The secondary mixture is directly ignited behind the blast bubble generated by the primary mixture. A curved oblique detonation is established (12.92 μs), which steepens and has become a planar detonation at 30.23 μs. By the end of the run two planar detonations in both channels run side by side (54.03 μs) and, essentially, form a single detonation. The measured wave speeds compare very well with the CJ speed of the mixture (Fig. 9(a)) and the transmitted wave angle slowly approaches 90 degrees (Fig. 9(b)).

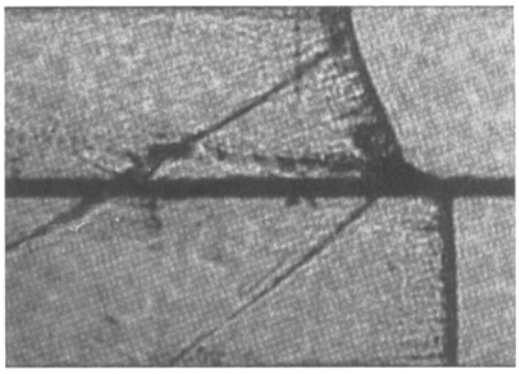

t = 32.8 μs.

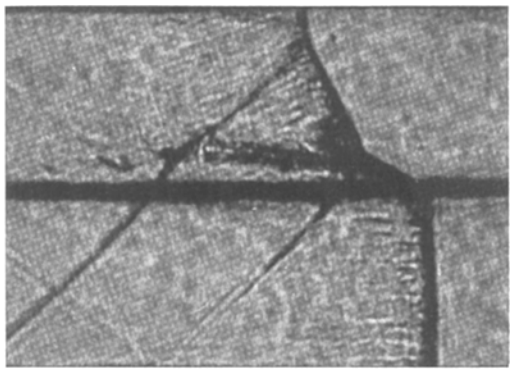

t = 52.23 μs.

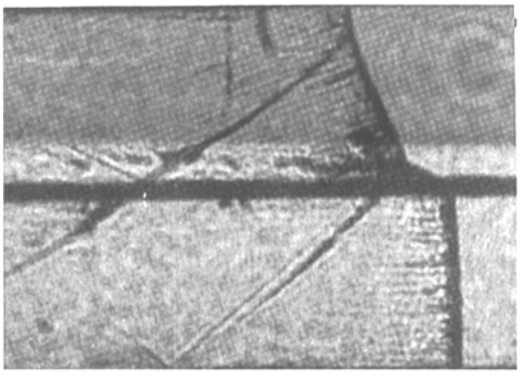

t = 34.9 μs.

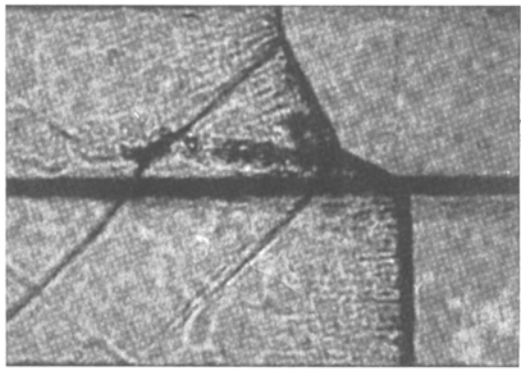

t = 54.4 μs.

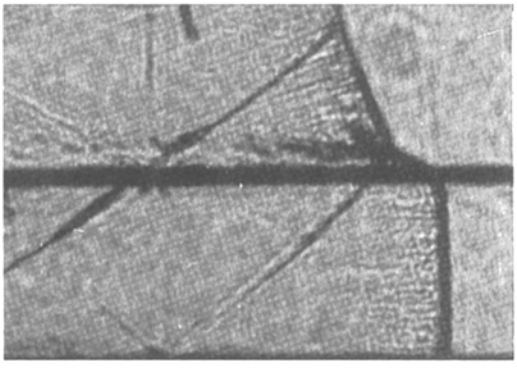

t = 37.08 μs.

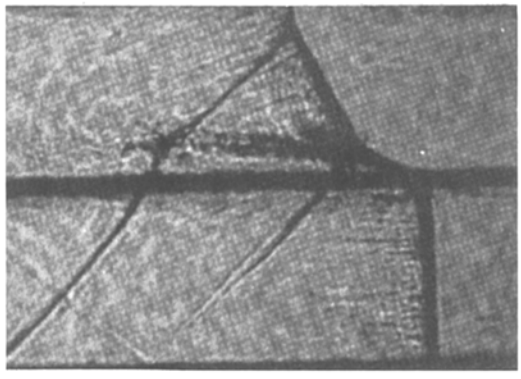

t = 56.6 μs.

Fig. 12. Schlieren photographs of the interaction; $\phi_1 = 1.5$, $\phi_2 = 0.7$

5.3 Rich primary / lean secondary

The Mach No. M_2 in the secondary mixture is now (Table 2) significantly higher than the Mach No. M_1 in the primary mixture. As a result, the nature of the diffraction and ignition in the secondary mixture is strikingly different from that observed when the primary mixture is lean.

The sketches and Schlieren framing photographs of the diffraction patterns when $\phi_1/\phi_2 = 1.0/0.45$ are shown in Fig. 10. Direct ignition behind the transmitted oblique shock was observed in all but two runs for this mixture combination. When direct ignition occurs, the flame front behind the blast wave, instead of detaching from the leading shock as in the lean / rich cases, now remains coupled to the shock, as is evident at 12.6 μs. The blast-bubble front has a wavy appearance, suggesting the possible presence of localized micro explosions. By the time this expanding bubble reaches the upper wall, at 15 μs, transition to an oblique detonation has started. This oblique detonation does not intersect

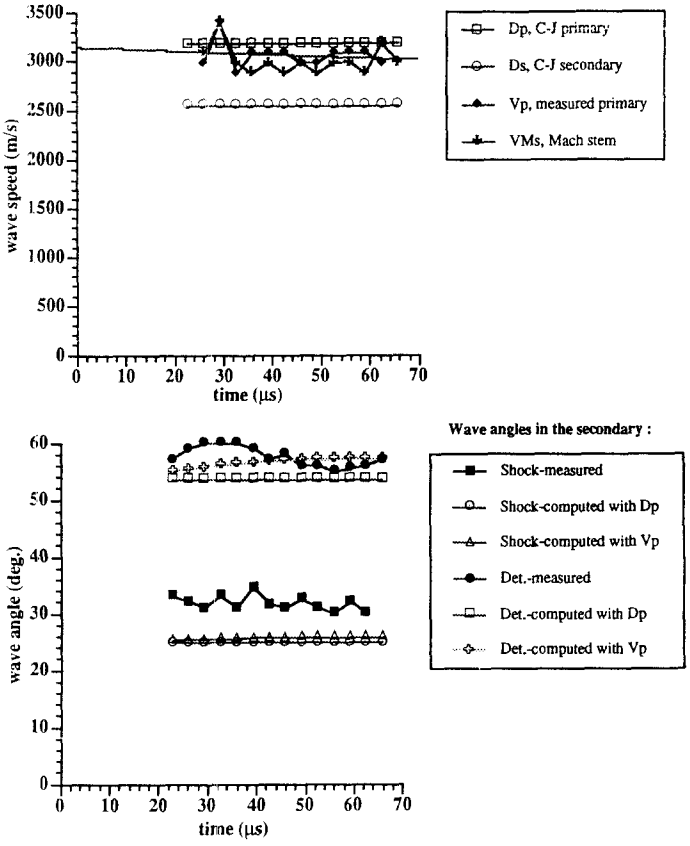

Fig. 13a,b. $\phi_1 = 1.5$, $\phi_2 = 0.7$. **(a)** Theoretical and measured wave speeds versus time; **(b)** measured and computed wave angles versus time

the primary detonation directly, but is connected to it by a short oblique shock segment. This oblique-shock oblique-detonation complex has been observed in many of the rich / lean experiments and is consistent with the shock-polar analysis discussed above.

By 22.2 μs Mach reflection of the oblique detonation from the upper wall is clearly visible, and a triple point has formed at the intersection of the transmitted oblique shock and the oblique detonation from which a shock is reflected back into the primary mixture. The oblique detonation is connected to this triple point by a small shock segment normal to the direction of propagation, and a slight uncoupling of the reaction front appears to occur there.

In the absence of direct ignition for $\phi_1/\phi_2 = 1.0/0.45$, a case which is not shown here, an oblique shock is transmitted into the secondary mixture. As in the lean / rich cases, ignition, then, occurs at the intersection of the reflected shock and the contact surface. The Mach stem at the upper surface then accelerates to becomes a plane detonation. The length of this Mach stem is small compared to the size of the oblique shock and appears to remain constant.

Wave speeds and angles are shown in Fig. 11 (a) and (b) for a run in which direct initiation was observed. With direct initiation, V_p, the measured speed of the primary wave, decreases slightly during the run. The measured values of the oblique detonation angles are always somewhat above the computed value during the period of observation but do approach the theoretical value toward the end. This result is consistent with the fact that the measured primary velocity $V_p < D_p$, the theoretical value. The oblique shock angle oscillates between 28 and 30 degrees, which correlates very well with the angles measured in the two runs for which direct ignition was not observed. The measured angle is slightly greater than the calculated value, again consistent with $V_p < D_p$.

The computed temperature T_{20} behind the transmitted oblique shock for $\phi_1/\phi_2 = 1.0/0.45$ is 698 K (Table 2) and the velocity is 2500 m/s. Behind a normal shock wave traveling at $D_p = 2841.5$ m/s, the temperature $T_{2n} = 2414$ K, the gas speed is 709 m/s, and the induction time is 0.02 μs. These results explain why direct initiation is possible for this equivalence ratio combination.

The framing sequence for $\phi_1/\phi_2 = 1.5/0.7$ is shown in Fig. 12. The secondary mixture is now ignited before the blast bubble reaches the top wall. Shortly thereafter, the oblique-shock oblique-detonation complex described above is established, and this basic configuration does not change throughout the rest of the run, 32.8 $\mu s < t < 56.6$ μs. The behavior at the triple point where the oblique shock and detonation meet is similar to that described above. A Mach stem, whose length remains constant, develops at the upper wall. As can be seen from Fig. 13(a), the speed V_p of the primary detonation and VMs, that of the Mach stem, are approximately equal and slightly below D_p, the CJ speed of the primary mixture, and the speeds decrease during the run. From Fig. 13(b) it can be seen that the oblique detonation angle is initially much greater than the computed value but then converges to the computed value toward the end of the run. In both runs, the shock and detonation angles converged to 28–30° and 60–58° respectively.

Experiments also were conducted for $\phi_1/\phi_2 = 2.0/0.57$ but are not reported in detail here. The results were similar to those of the other rich primary / lean secondary experiments.

Conclusions

Experiments were performed in a layered shock-tube, with H_2-O_2 mixtures of different equivalence ratios in the two explosive layers. The Chapman-Jouguet detonation speed of the primary mixture was increased while that of the secondary mixture was decreased. Measured shock velocities and angles were compared to values computed using steady-state shock and detonation theory.

In the lean primary / rich secondary cases, the primary mixture was not energetic enough for the secondary mixture to ignite directly behind the blast wave transmitted into the secondary explosive. Two modes of detonation ignition were then observed. At the lower values of the primary detonation velocity D_p, an oblique shock was transmitted into the secondary mixture. Although the secondary gas was heated as it passed through the oblique shock, the temperature was too low for ignition. Instead, when the oblique shock angle was such that Mach reflection occurred at the test section top wall, the secondary gas ignited behind the Mach stem. When regular reflection took place, the gas was observed to explode along and behind the reflected shock, where it crossed the density interface behind the oblique shock. As a result of the explosion, a blast wave was generated which steepened the reflected shock, resulting in the formation of a Mach stem behind which combustion occurred. These two

modes of ignition also have been observed in numerical experiments with H_2-O_2-Ar mixtures.

In the rich primary / lean secondary cases, the primary detonation was generally strong enough for the secondary mixture to ignite behind the blast bubble. Direct ignition resulted in the rapid formation of an oblique-shock oblique-detonation wave combination or complex in the secondary mixture. When direct ignition did not take place, the transmitted wave structure consisted of a reactive oblique shock with a Mach detonation reflection at the top wall.

Combined oblique-shock oblique-detonation structures also were encountered in the numerical experiments of Li et al. (1995), who simulated the flow of an H_2-O_2-Ar mixture at Mach 8 over a 23 degree angle wedge. In the present layered shock-tube experiments, the slipstream between the burned primary and the shocked secondary mixtures actually acts as a wedge driven past the secondary mixture at the Chapman-Jouguet speed of the primary mixture, which thus parallels the configuration simulated by Li et al. (1995). An explanation for this combined shock-detonation structure is that the residence time of fluid particles near the leading edge of the wedge is too short for combustion reactions to occur, and that time is sufficient for combustion only further away from the leading edge, where, then, a detonation is possible. Shock-polar analysis also suggests this type of structure.

The accuracy of the two-gamma method in predicting wave patterns depends on how close the observed diffraction is to steady state. Computing the characteristic time to reach steady state as the time it takes for a sound wave to travel from the interface to the top shock tube wall and back, this is found to be 40 to 70 μs. This value actually correlates well with the plots of wave angles versus time, which show that, in many cases, experimental values tend to converge to the calculated ones in elapsed times of this order. In many cases, the steady-state values provide a reasonable estimate of the local properties of the diffraction, although a complete analysis will require appropriate numerical simulations of this complex diffraction process. It is hoped that the results presented here will provide a data base for evaluating such simulations.

Acknowledgement. Part of the work reported here was supported by The U.S. Army Research Office under grant No. DAAL03-87-K-0019, Dr. D.M. Mann, project monitor.

References

Ben-Dor G (1978) Regions and Transitions of Non-Stationary Shock Wave Diffractions in Perfect and Imperfect Gases, UTIAS Report No. 232

Dabora EK (1963) The Influence of a Compressible Boundary on the Propagation of Gaseous Detonations, Ph.D Thesis. The University of Michigan, Ann Arbor, Michigan

Dabora EK, Desbordes D, Guerraud C, Wagner HG (1991) Oblique Detonation at Hypersonic Velocities. In: Kuhl AL (ed) Dynamics of Explosions and Explosions: Detonations, Progress in Aeronautics and Astronautics. AIAA 133:187–201

Getzinger RW, Schott G (1973) Physical Chemistry of Fast Reactions. In:Levitt BP (ed) Physical Chemistry of Fast Reactions vol. 1; chap 2, 81–160

Gordon S, MacBride BJ (1971) Computer Program for Calculation of Complex Chemical Equilibrium Compositions, Rocket Performance, Incident and Reflected Shocks and Chapman-Jouguet Detonations, NASA SP-273, National Aeronautics and Space Administration, Washington, DC

Gvozdeva LG (1961) Refraction of Detonation Waves upon Incidence on the Interface of Gaseous Mixtures. ZhTF 31: No.6 pp 731–739

Gvozdeva LG, Predvoditeleva OA (1969) Investigation of Triple Configurations of Detonation Waves in Gases. Fizika goreniya i vzryva 5: 451–461

Jones DA., Sichel M., Oran ES (1995) Reignition of Detonations by Reflected Shocks, Shock Waves 5: 47–57

Lee JH, Glass II (1984) Pseudo-Stationary Oblique-Shock-Wave Reflections in Frozen and Equilibrium Air. Prog. Aerospace Sci. 21:33–80

Li C, Kailasanath K, Oran ES, Landsberg AM, Boris JP (1995) Dynamics of Oblique Detonations in Ram Accelerators, Shock Waves 5: 97–101

Liou, JJ (1986) Analysis of the Wave Interaction Between a Propagating Gaseous Detonation and a Bounding Explosive Layer, Ph.D. Thesis. The University of Michigan, Ann Arbor, Michigan

Liu JC, Liou JJ, Sichel M, Kauffman CW, Nicholls JA (1986) Diffraction and Transmission of a Detonation into a Bounding Explosive Layer. 21st Symposium (International) on Combustion

Oran ES, Jones DA, Sichel M (1992) Numerical Simulations of Detonation Transmission, Proc. R. Soc. Lond. A 436: 267–297

Sommers WP (1961) The Interaction of a Detonation Wave with an Inert Boundary, Ph.D Thesis. The University of Michigan, Ann Arbor, Michigan

White DR, Moore GE (1967), Eleventh Symposium (International) on Combustion. The Combustion Institute, Pittsburgh, p. 147